Journal of Colloid and Interface Science 493 (2017) 150–161

Contents lists available at ScienceDirect

Journal of Colloid and Interface Science

journal homepage: www.elsevier.com/locate/jcis

Regular Article

Simple fabrication of zeolitic imidazolate framework ZIF-8/polymer composite beads by phase inversion method for efficient oil sorption

Zahra Abbasi [a], Ezzatollah Shamsaei [a], Xi-Ya Fang [c], Bradley Ladewig [a,b], Huanting Wang [a,*]

[a] Department of Chemical Engineering, Monash University, Clayton, Victoria 3800, Australia
[b] Barrer Centre, Department of Chemical Engineering, Imperial College London, London SW7 2AZ, United Kingdom
[c] Monash Center for Electron Microscopy, Monash University, Clayton, Victoria 3800, Australia

GRAPHICAL ABSTRACT

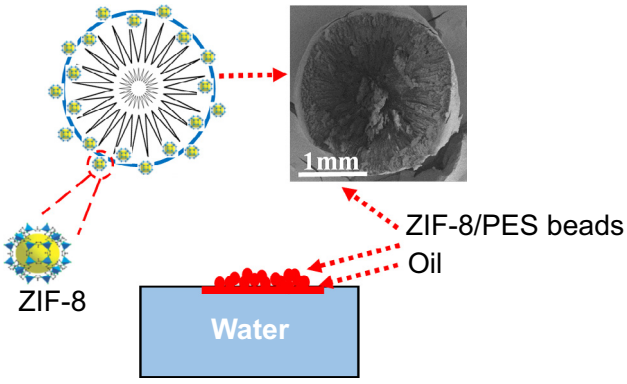

ARTICLE INFO

Article history:
Received 11 November 2016
Revised 1 January 2017
Accepted 3 January 2017
Available online 5 January 2017

Keywords:
Oil sorption
Metal organic framework
ZIF-8
Composite beads
Water treatment

ABSTRACT

Zeolitic imidazolate framework ZIF-8 beads of 2–3 mm in diameter were prepared using a simple one-step phase inversion method. The beads were fabricated by different amounts of ZIF-8 to polyether sulfone (PES) ratios. ZIF-8 played the role of an adsorbent while PES acted as a binder in the composite matrix to keep the ZIF-8 particles. Since ZIF-8 is highly hydrophobic, the beads floated on water and adsorbed oil droplets successfully. This efficient oil adsorption is attributed to the hydrophobicity and high surface area of ZIF-8 particles which can effectively adsorb oil droplets. Different characterization techniques were used to understand the textural properties of the composite beads. The FESEM analysis showed that ZIF-8 particles were well coated and dispersed into the polymer bead composites and some pores are created on the beads surface at higher loadings which facilitated high oil sorption. The nitrogen adsorption-desorption indicated that ZIF-8/PES beads had very high surface area which makes them suitable for adsorption applications. The ZIF-8/PES beads demonstrate easy handling and recycling compared to ZIF-8 powder and showed superior buoyancy and oil sorption capacity compared with natural sorbents like activated carbon. This study shows the phase inversion method can be applied to produce a variety of functional composite bead materials for specific applications like adsorption.

* Corresponding author.
E-mail address: huanting.wang@monash.edu (H. Wang).

http://dx.doi.org/10.1016/j.jcis.2017.01.006
0021-9797/

1. Introduction

Oil spillage and industrial organic pollution have become serious environmental issues around the world which pose threats to human health as well as the ecosystem [1–4]. Oil contamination can result in the increase of biochemical oxygen demand (BOD) and chemical oxygen demand (COD) causing serious environmental hazards [5]. As a result, great attention has been paid to the development of efficient and cost-effective approaches to cleaning up oil spillage, especially where it occurs in water bodies [3].

Among the various different approaches, adsorption has the advantage of being simple and cost effective with the ability of removing different types of contaminants form water [6]. Natural adsorbents such as activated carbon [7] and natural zeolites [8] have been shown to be somewhat effective in oil removal. Although these natural sorbents have the advantage of being economic, they have the limitation of low oil sorption capacity, low hydrophobicity and poor buoyancy [9]. Therefore, many efforts have been made to tackle the issue of oil spillage pollution by developing efficient adsorbents like microporous polymers [10–12], carbon-nanotube (CNT) [13], graphene [1] as well as carbon soot sponge [2], graphene aerogel [14] and macroporous carbon nanofiber film [15]. A universal and consistent drawback of these materials is their complex synthesis procedures and they usually require surface modification before oil adsorption which restricts their practical applications. For example, in the synthesis of spongy graphene, it is required to prepare graphene oxide by oxidizing expandable graphite under 98 wt.% sulphuric acid and potassium permanganate solution at 98 °C [1] which is very dangerous. In addition, for preparation of carbon nanofiber oil sorbent, the coating of the material by polydimethylsiloxane is needed prior to application in oil adsorption [16].

Different kinds of monodisperse composite spheres have been employed in separation [17], drug delivery [18] catalysis [19] as well as adsorption [20] due to their high surface area and porous structure. However, millimetre sized spheres and beads are much easier to handle and recover compared with smaller scale (like nano scale) spheres. To date, there have been several attempts to produce beads and spheres using different techniques. For example, a templating technique involving high internal phase emulsions (HIPEs) has been developed for producing monodisperse emulsion-templated polymer beads via sedimentation polymerization. Nevertheless, this technique has a number of limitations including utilization of alkoxide precursors which are highly reactive to water and should be separated before formation of oil-in-water emulsion. Moreover, it is likely that the emulsion converts to gel before the injection process is completed [21]. In addition, this method includes several steps like immersion of polymer bead scaffolds into inorganic precursor, filtration, gelation and calcination. These steps make the process complicated and time consuming. Therefore, since the existing preparation methods are very complicated, an easy and straight forward method was established to prepare millimetre-sized beads.

Phase inversion is a common method for preparation of asymmetric membranes. This method has been utilized in our group to synthesize porous hollow fiber membrane [22], nanocomposite ultrafiltration membrane [23], hollow carbon beads for oil sorption [24], and zeolitic imidazolate framework ZIF-8 polymer spheres for gas adsorption [25].

Metal organic frame works (MOFs) are a group of porous materials composed of a metal ion or a cluster of metal ions and an organic molecule which is called a linker. MOFs have high porosity and open metal sites which makes them suitable for different applications specifically for adsorptive removal of contaminates from water [26]. Zeolitic imidazolate frameworks (ZIFs) are a category of MOF materials which exhibit satisfying chemical and thermal stability. ZIF-8 is one of the most studied ZIF materials with the formula of Zn(2-methylimidazole)$_2$ with a sodalite zeolitic structure. ZIF-8 has pore size of 1.1 nm and accessible pore window of 0.34 nm which has been investigated for a variety of applications such as adsorption, separation and catalytic applications [27–30]. Furthermore, ZIF-8 has been extensively studied for the adsorptive removal of pollutants from water [27,31–35] since it is amongst the most stable metal organic frameworks. Recently, ZIF-8 particles in the form of powder have been utilized for adsorption of oil droplets from water [36].

Metal organic frameworks are generally prepared as powders which are not suitable for many practical applications including adsorption and catalysis. Therefore, shaping these materials is required for easy handling and recycling [37]. HKUST-1 MOF has been shaped as beads by coating onto polymer and oxide composite beads [37]. SIM-1 (an isostructural to ZIF-8) was coated on spherical alumina beads [38]. However, the methods utilized for coating MOF on the beads require high temperatures like 85 °C for 48 h [38].

In this work we demonstrate a simple, fast and one step method at room temperature for fabricating ZIF-8 particles into polymer beads using a phase inversion method. The beads prepared by this method are very easy to handle and recover from oil-water mixture compared to ZIF-8 powder. ZIF-8/PES composite beads exhibited efficient oil sorption and they are amongst the best sorbent materials previously reported; especially in comparison with natural common sorbents like activated carbon as well as other synthesized beads.

2. Materials and methods

2.1. Materials

Zinc nitrate hexahydrate ($Zn(NO_3)_2{\cdot}6H_2O$), 2-methylimidazole (Hmim), 1-methyl-2-pyrrolidone (NMP) (99%), toluene, paraffin oil, olive oil and oil red were purchased from Sigma Aldrich. *n*-Hexane was purchased from Merck. Polyethersulfone (PES) was supplied from BASF Company. All chemicals were used as received without further purification.

2.2. Synthesis of ZIF-8 nanocrystals

ZIF-8 was synthesized by a synthesis method reported by Koji Kida et al. [16] in aqueous solution. 0.744 g (2.5 mmol) of $Zn(NO_3){\cdot}6H_2O$ and 12.3 g (0.15 mol) of Hmim were dissolved in 10 ml and 90 ml of deionized water respectively and stirred for 24 h. ZIF-8 nanocrystals were collected by washing with methanol and centrifuging (8000 rpm, 15 min) for three times and then dried at 60 °C overnight.

2.3. Preparation of polyethersulfone spheres and ZIF-8/PES composite beads by phase inversion method

Typically, 1 g of polyethersulfone was dissolved in 5.5 g NMP under magnetic stirring at room temperature overnight. The polymer solution was vertically pumped into water with an air gap (the distance between the needle tip and water surface) of about 4 cm. The flowrate of the polymer solution was set at 0.2 ml/min and the syringe tip was 18 G (inner diameter of roughly 0.84 mm). Solid polymer spheres were formed in water immediately through solvent/water exchange and kept in water overnight for further solvent/non-solvent exchange. Then formed PES spheres were dried at 80 °C overnight.

ZIF-8/PES composite beads were made by the same method except that a syringe tip with 14G (inner diameter of roughly 1.6 mm) size was used. ZIF-8/PES composite beads were prepared by ZIF-8: PES ratios of 0.5, 1, 2 and 4. The ZIF-8/polymer slurry was viscous and the resulting beads were oval in shape as with the ZIF-8: PES ratio of 4. It is worth mentioning that for higher loadings of ZIF-8, i.e. for ZIF-8: PES ratios of 2 and 4, the amount of NMP solvent increased to 8 and 10.5 g respectively. Moreover, for ZIF-8/PES-2 and ZIF-8/PES-4, the air gap had to be increased to double (8 cm) in order to be able to form the ZIF-8/PES beads in the water tank.

2.4. Characterization

Nitrogen adsorption and desorption isotherms were measured at liquid nitrogen temperature (77 K) using an accelerated surface area and porosimetry system (ASAP 2020, Micromeritics, USA) for surface area measurements. The pore size distributions of ZIF-8 powder and ZIF-8/PES composite beads were measured by nitrogen sorption using ASAP 2020. However, the pore size distribution for PES spheres was analysed by mercury porosimetry (AutoPore IV 9500 mercury porosimeter, Micromeritics, USA). The crystal structures of the samples were identified using an X-ray diffractometer (Miniflex 600, Rigaku) with Cu Kα radiation at 40 kV and 20 mA over the 2θ range of 5–40°. The morphology of the adsorbent materials was observed using a scanning electron microscope (FEI Nova NanoSEM 450 FEG SEM). The water droplet contact angle measurement was carried out at room temperature with 1 μL water droplet on the film of samples using contact angle goniometer (Dataphysics OCA15, Dataphysics, Germany). A film of the sample was made by manual pressing. An attenuated total reflectance (ATR) Fourier Transform Infrared (FTIR) (Perkin Elmer, USA) was used to collect the FTIR spectra of the samples in the range of 500–4000 cm^{-1} at an average of 32 scans with a resolution of 4 cm^{-1}.

2.5. Oil sorption experiments

For oil adsorption capacity measurement, the composite beads were immersed in several oils and organic compounds including paraffin oil, olive oil, toluene and *n*-Hexane for half an hour. Then the beads were wiped to remove the extra oil or organic compound on the surface and then weighed very quickly by a balance to minimize errors arising from solvent evaporation. The amount of adsorbed oil (the volume percentage of oil adsorbed on the composite beads) was calculated as follows:

$$Volume\ gain(\%) = \frac{(W_S - W_C)}{W_C} \times \frac{\rho_C}{\rho_O} \times 100\%$$

where W_s is the weight of ZIF-8 composite beads after oil adsorption and W_c is the initial weight of the beads before adsorption. ρ_c is the bulk density of ZIF-8/PES beads and ρ_o is the oil density.

The composite beads were regenerated by simple washing with ethanol to assess the recyclability of the prepared beads. The used oil-rich beads were added to ethanol and mixed for a few hours. The regenerated beads were dried at 70 °C and tested for subsequent oil sorption experiments.

3. Results and discussions

3.1. Characterization of ZIF-8/PES composite beads

The XRD analysis on ZIF-8 beads was done to investigate the incorporation of ZIF-8 particles into the polymer (PES) framework. The X-ray diffraction patterns (Fig. 1) confirms the existence of ZIF-8 particles in the matrix of the polymer composite beads. All of the composite beads exhibit the diffraction patterns similar to that of pure ZIF-8 powder shown in Fig. 1. It is apparent that by increasing the ZIF-8 loading the corresponding XRD peaks intensity also increases. This also shows that ZIF-8 particles are dispersed within the beads matrices and this is consistent with SEM results.

Fig. 2 shows the morphology of the top surface of the beads indicating that ZIF-8 particles are coated and dispersed on the outer surface of the beads. It is evident from the figure that the outer surface of the composite spheres are covered by ZIF-8 particles and the coverage becomes more pronounce as the ZIF-8 loading increases. For the PES spheres the outer surface of the beads are very smooth without any particles on the surface. As the ZIF-8 loading increases, the top surface contains more ZIF-8 particles. As ZIF-8 particles migrate to the surface, large pores are created at the outer surface of the composite bead. Apart from the creation of large pores on the surface, the polymer keeps the ZIF particles together very uniform in the composite texture. This results in more exposure of the ZIF particles to the oil and organic molecules and leads to a higher performance. The creation of the large pores on the surface also facilitates the pollutant absorption and diffusion into the composite bead framework.

For investigation of the inner structure of ZIF polymer composite beads, a single bead was cut into half. From the cross sectional images it can be seen that ZIF-8 particles are fully dispersed within the pores of the polymer framework. Fig. 3 shows the coverage at different magnifications. The cross section of the ZIF-8/PES beads shows a very porous structure with large channels of macrometer sizes which are covered by ZIF-8 particles. The ZIF-8 particles are distributed inside the pores and have the diameter of about 250 nm. The macropores inside the beads facilitate ZIF-8 incorporation in the beads matrices. As can be seen from the SEM images, ZIF-8 particles are fairly well distributed among the channels and inside the pores. The porous framework within the polymer matrix consists of large micrometre pores which were created during the phase inversion process. Fig. 4 shows the inversion process and how the macrometer pores are created in the polymer sphere during this process.

Nitrogen adsorption-desorption isotherms at 77 K for the composite beads are shown in Fig. 5. As can be seen from Fig. 5 the surface areas of the composite beads increased with raising the loading of ZIF-8 powder into the polymer matrix. Therefore, the adsorption capacities of the oil and organic compounds increased accordingly. ZIF-8 is well-known for having very high surface area (1384.2 m^2/g BET and 1849 m^2/g Langmuir surface area) as reported in Table 1. With increasing the loading of ZIF-8 particles in the polymer composite, the BET surface area increases as 343.2, 602, 882.3 and 1030.6 for ZIF/PES-0.5, ZIF/PES-1, ZIF/PES-2 and ZIF/PES-4 respectively. ZIF/PES-4 has the highest surface area among the polymer composite beads and the surface area is very close to the pure ZIF-8 powder's surface area. ZIF/PES-4 exhibits the highest adsorption capacity for all the oil and organic model compounds which can be attributed to the very high surface area as well as its high pore volume. The pore size distributions are demonstrated in Fig. 5. The ZIF-8/PES beads exhibit pore size distributions similar to ZIF-8.

The pore size distribution of the PES beads was defined using the mercury intrusion porosimetry to analyse the macroporous structure of the PES beads, since the nitrogen sorption analysis is only applicable for microporous and mesoporous materials. Therefore, the pore size distribution of ZIF-8 was determined by nitrogen adsorption-desorption analysis but for PES spheres, mercury porosimetry was utilized. The macro metre pore size distribution of PES spheres is shown in Fig. 6. The macropore size from the mercury porosimetry is defined in the range of 1–3 μm which is consistent with the SEM results (Fig. 3).

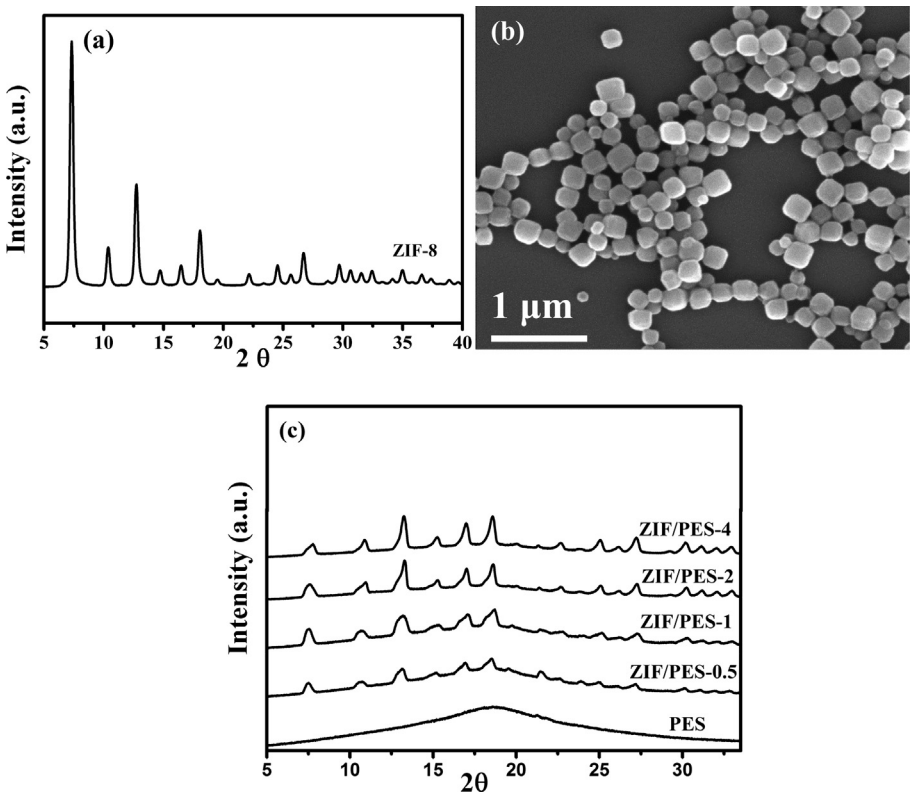

Fig. 1. XRD pattern (a) and SEM image (b) of ZIF-8 nanocrystals and XRD patterns of PES polymer and ZIF-8/PES composite beads with different loadings (c)

FTIR spectra of ZIF-8/PES beads were very similar to the pure ZIF-8 (Fig. 7). The peaks at 3135 and 2929 are characteristic of aromatic and aliphatic C—H stretch of imidazole while the peaks observed at 1584 and 800–1500 (759, 1145, 1306 and 1444) are assigned to C═N stretch mode and entire imidazole ring vibrations mode, respectively [39].

3.2. Oil sorption of ZIF-8/PES composite beads

The bulk densities of the ZIF-8/PES composite beads were calculated as 0.035, 0.053, 0.173, 0.1875 and 0.2657 g/cm^3 corresponding to PES, ZIF/PES-0.5, ZIF/PES-1, ZIF/PES-2 and ZIF/PES-4 respectively as shown in Table 2. The very low bulk density allows the beads to float easily on the surface of water. Consequently, these ZIF-8/PES composite beads are evaluated as sorbents for oil spillage clean-up.

The ZIF-8/PES composite beads with various loadings are shown in Fig. 8. It can be seen that by increasing the ZIF-8 loading, the shape of the beads changes from spheres to ovals. The diameter of the PES beads and ZIF-8 composite beads are 1–2 mm and 2–3 mm respectively. To demonstrate ZIF-8/PES beads adsorb oil efficiently, paraffin oil which was labelled with oil red was poured on the surface of water. Then ZIF-8/PES composite beads were gently placed on the surface of oil-water as illustrated in Fig. 9. The figure shows that composite beads absorb oil efficiently from the surface of water.

The oil adsorption capacity depends on the hydrophobic nature of the adsorbent since oil droplets are hydrophobic in nature. Thus hydrophobic interaction between the oil molecules and the adsorbent surface facilitates the oil sorption process. It is believed that the suitable oil sorbent is required to be hydrophobic. Improving hydrophobicity of the sorbent surface will enhance the van der Waals force and hydrophobic interaction between oil droplets and sorbent materials which leads to high sorption capacity. Sorbent materials are also required to have high surface area and porosity to offer adequate surface sorption sites for catching oil molecules [40]. Several oils and organic solvents were used to examine the saturated oil sorption capacities of the ZIF-8/PES composite beads for different kind of pollutants and the results are presented in Fig. 11. It can be seen that the composite beads have more tendency to adsorb paraffin and olive oil rather than *n*-Hexane and toluene organic solvents. The ZIF-8/PES beads with ZIF-8: PES ratio of 4, can adsorb up to 37.6% of their volume for paraffin oil while the corresponding uptake for olive oil is 35.6%. The corresponding uptakes for the composite beads with the ZIF-8: PES ratios of 0.5, 1 and 2 were 6.5, 10.2 and 24.9% for paraffin oil and 3.2, 8.5 and 18.9% for olive oil respectively.

ZIF-8 has been reported to be a highly hydrophobic microporous material [41–44]. The hydrophobicity of ZIF-8 has been investigated and proved by water adsorption [42]. This hydrophobicity is attributed to its chemical composition i.e. the methyl-functionalized *Im* linkers as well as the coordinative saturation of the metal sites. Typically, ZIF materials can have hydrophobic framework if the *Im* linkers do not consist of hydrophilic functionalities [41]. The increasing of the ZIF-8 loading in the composite beads framework, results in a large amount of ZIF-8 particles to be present on the beads surfaces (refer to the SEM image in Fig.3). This feature is further confirmed by the water contact angle measurement shown in Fig. 10. The water contact angle of the samples was measured, and the left and right angles of ZIF-8 powder were 120 and 118°, respectively as shown in Fig. 10(a). The left and right contact angles of ZIF/PES-4 composite beads were determined to be 100 and 115°, respectively as can be seen from Fig. 10 (b). Thus, increasing the ZIF-8 loading helps to benefit from both hydrophobicity and high surface area of ZIF-8 particles for oil adsorption. Therefore, we can observe much higher adsorption properties for the highest ZIF-8 loading (ZIF/PES-4) compared to lower ZIF-8 loadings and PES spheres.

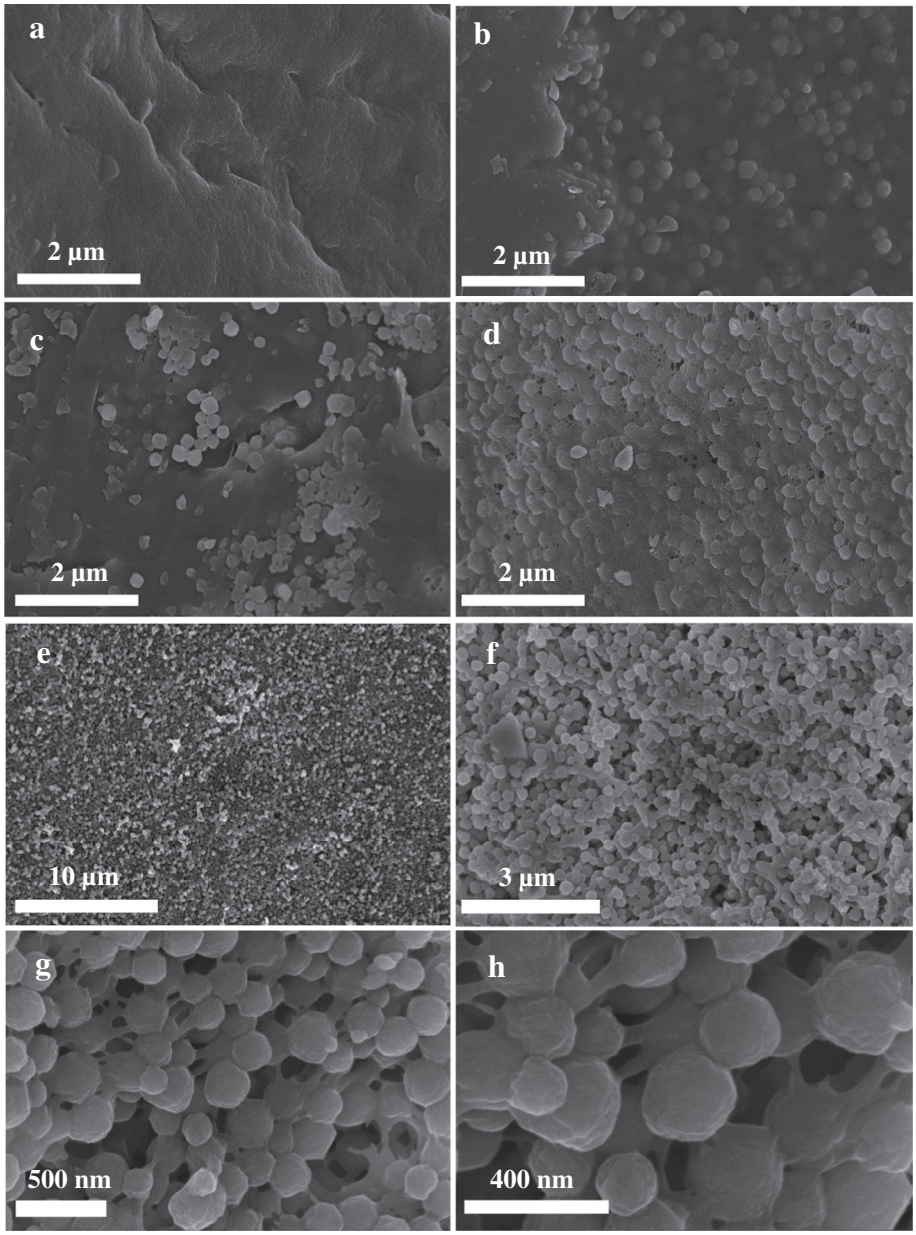

Fig. 2. Top-surface SEM images of PES (a), ZIF/PES-o.5 (b), ZIF/PES-1 (c) and ZIF/PES-2 (d). The images (e-h) show the top surface of ZIF/PES-4.

The hydrophobic interactions between ZIF-8 and hydrophobic chains of oil molecules result in the adsorption of oil compounds on the surface of ZIF-8/PES composite beads. In order to understand the reason behind the difference in oil adsorption capacity amongst the ZIF-8/PES beads, the morphologies, surface areas and the pore size distributions of the composite beads were investigated.

The performance of ZIF-8 composite beads is shown in Fig.11. As shown in the figure, all the ZIF-8/PES beads show the highest sorption for paraffin oil followed by olive oil, *n*-hexane and toluene. It is observed that increasing the ZIF-8 loading for ZIF/PES-2 and ZIF/PES-4 rises the sorption capacity dramatically. For example, for paraffin oil, the sorption capacity raises from 6.5 and 10 percent (volume gain) for ZIF/PES-0.5 and ZIF/PES-1 to 24.9 and 37.6 percent for ZIF/PES-0.2 and ZIF/PES-4. The equivalent sorption capacity (weight basis) for ZIF/PES-4 is calculated as 1260 mg/g which is quite high in comparison with most natural sorbents like activated carbon (Table 3). The high sorption capacity could be due to the high surface area of the composite beads as well as the created pores on the surface which is the result of large amount of ZIF-8 particles movement toward the outer surface of the polymer composite beads. These pores offer little resistance to diffusion of the oil molecules into the sphere, increasing the adsorption capacity.

From Fig. 11 it can be seen that ZIF-8/PES beads have a high tendency to adsorb *n*-Hexane. The critical diameter[1] of *n*-hexane is 0.43 nm [45]. ZIF-8/PES composite beads adsorb *n*-hexane up to 30.2 percent of their volumes for the ZIF/PES-4. The high adsorption capacity of ZIF-8 for *n*-hexane is in accordance with the findings in literature [45]. It is worth noting that the adsorption of *n*-hexane might have been underestimated since it has a low boiling point of 68 °C and evaporates rapidly. To explore the ZIF-8/PES composite beads' capacities for the adsorption of branched organic molecules,

[1] The critical diameter refers to the smallest cross-sectional diameter of the molecule.

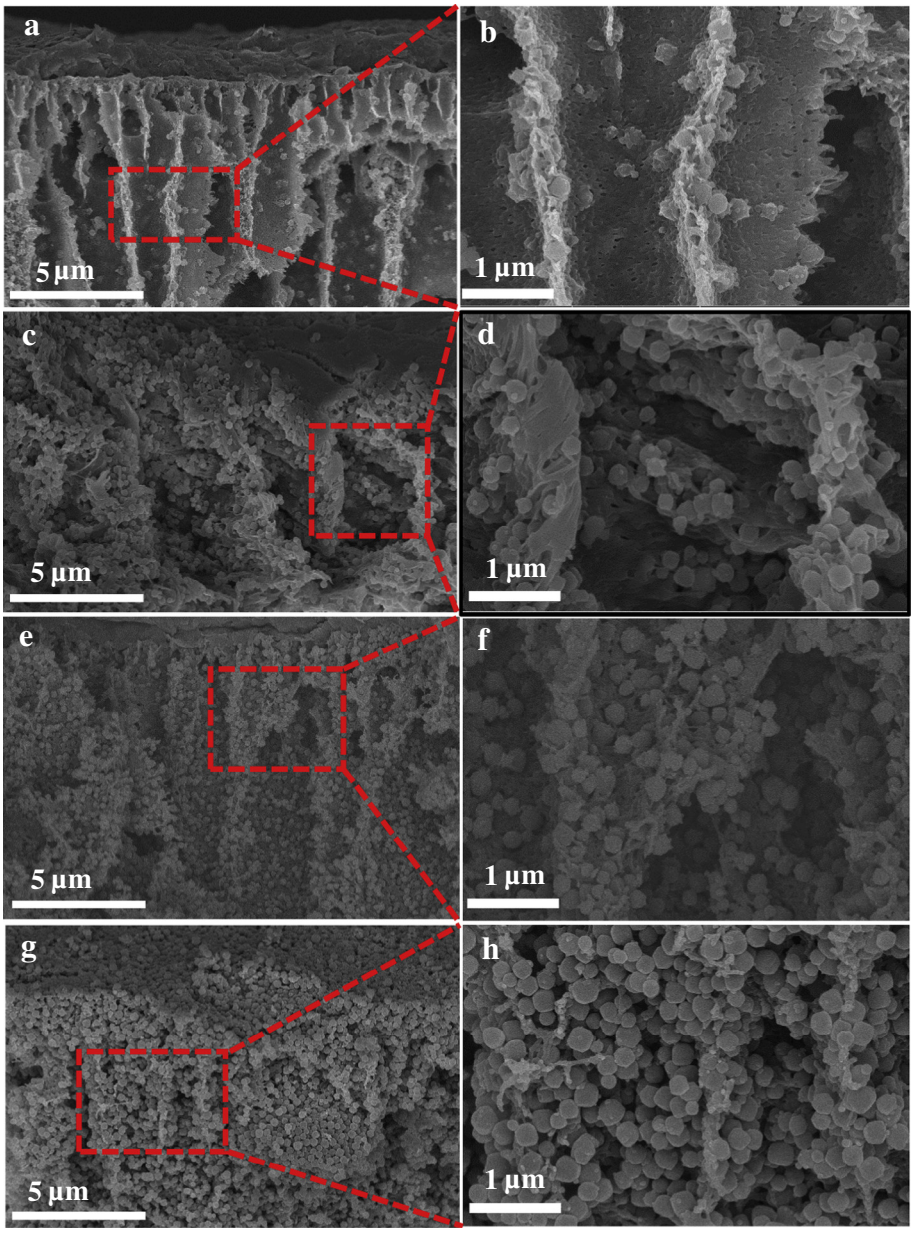

Fig. 3. Cross sectional SEM images of ZIF/PES-o.5 (a, b), ZIF/PES-1 (c, d), ZIF/PES-2 (e, f) and ZIF/PES-4 (g, h).

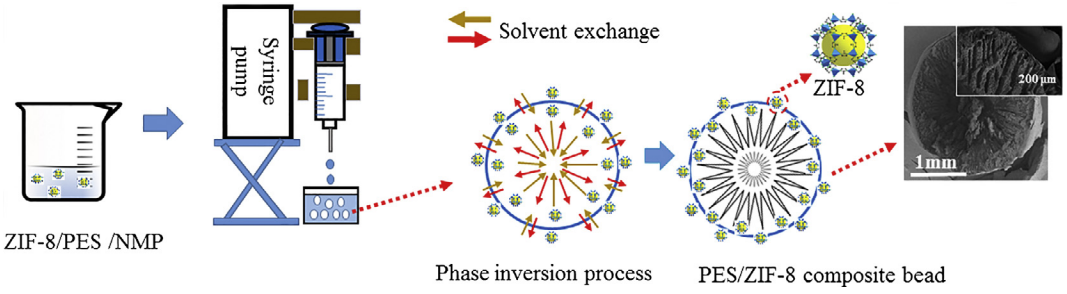

Fig. 4. Schematic illustration of formation of ZIF-8/PES composite beads via phase inversion and the creation of porous framework

toluene was used as an aromatic molecule in this study. In contrast with what has been reported in literature, we found the ZIF-8/PES beads have fairly moderate tendency to adsorb toluene. It has been reported that toluene (kinetic diameter of 0.58 nm) cannot enter and diffuse into the microporous structure of ZIF-8 (with accessible pore size of 0.34 nm) [46,47]. ZIF-8 was reported to have almost nil adsorption capacity for toluene. In another study it was declared that branched alkanes cannot penetrate the pores of ZIF-8 [48]. However,

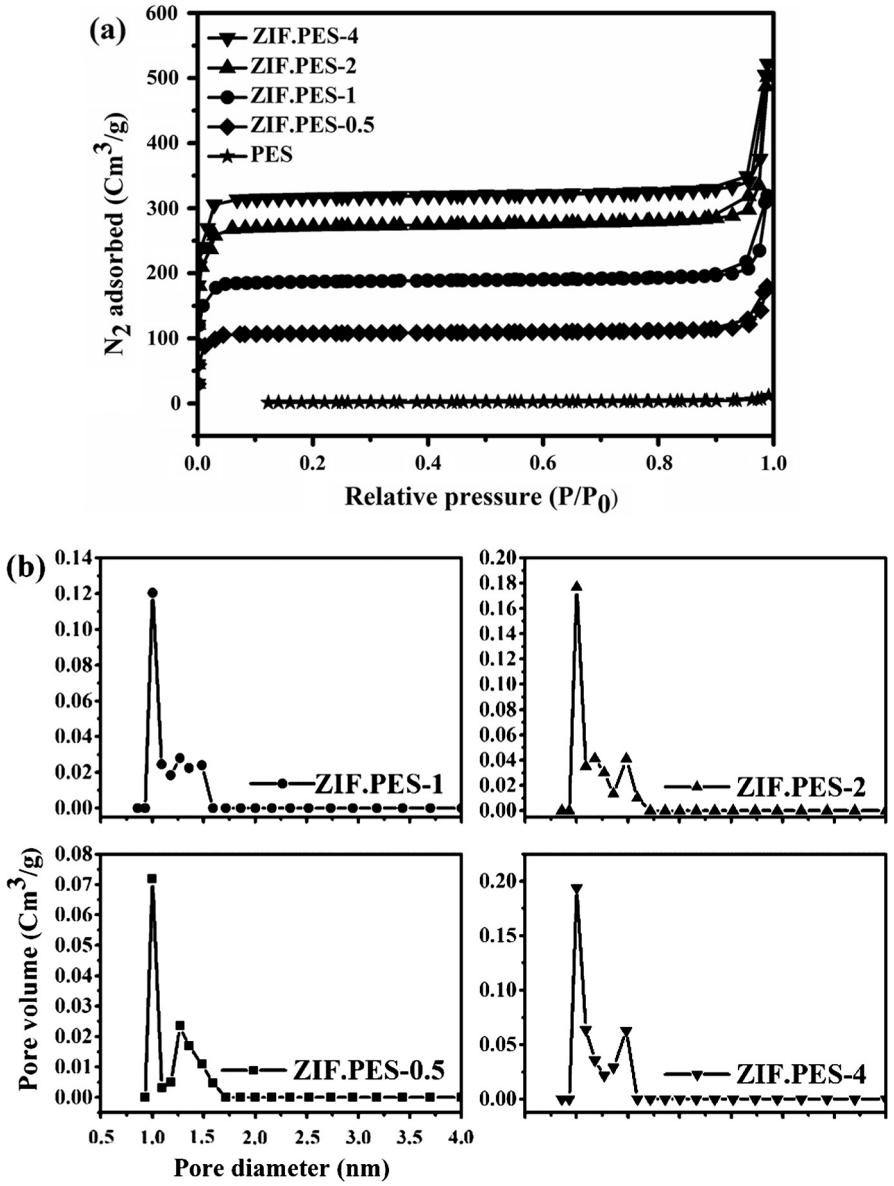

Fig. 5. Nitrogen adsorption-desorption isotherm of PES and ZIF-8/PES composite beads (a) and the pore size distributions for ZIF-8/PES composite beads (b).

Table 1
Surface area analysis parameters of ZIF-8, PES and ZIF-8/PES composite beads.

Sample	BET surface area ($m^2.g^{-1}$)	Langmuir surface area ($m^2.g^{-1}$)	Total pore volume ($cm^3.g^{-1}$)[a]	Micropore volume ($cm^3.g^{-1}$)
ZIF-8	1384.2	1849	1.1	0.63
ZIF/PES-4	1030.6	1382	0.81	0.47
ZIF/PES-2	882.3	1185.2	0.77	0.4
ZIF/PES-1	602	814.8	0.49	0.27
ZIF/PES-0.5	343.2	470.8	0.27	0.16
PES	0.6	NA	0.01	0.0

[a] At P/P0 = 0.99.

in our study we report that ZIF-8 composite beads show fairly high adsorption capacity for toluene which might be due to the formation of large pores on the top surface of the composite beads at higher ZIF-8 loadings. There are similar reports in the literature which show ZIF-8 has the potential to adsorb the molecules larger than the ZIF-8 pore opening. Adsorption of benzene [45] and *p*-xylene [49] in liquid

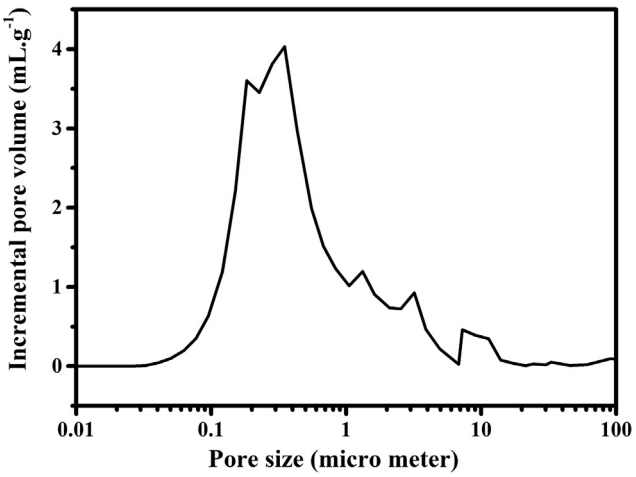

Fig. 6. Mercury porosimetry curve of PES.

phase on ZIF-8 has been reported. The investigations showed that ZIF-8 is capable of adsorbing benzene and *p*-xylene although the kinetic diameters of these molecules are much larger than the pore size of ZIF-8 particles. Benzene, toluene and *p*-xylene have the kinetic diameters of 0.58 nm [50] which is almost twice the ZIF-8 aperture size and ZIF-8 tendency for adsorption of these molecules show the flexibility of ZIF-8 structure. It was also stated that ZIF-8 adsorbs organic molecules in the order of alkane > alkene > aromatic [49] which was confirmed in this study, as *n*-hexane adsorbed at much higher levels than toluene as an aromatic compound.

The difference in the oil and organic sorption can be related to the viscosity and surface tension of the oil and organic compounds as well. Viscosity can affect the sorption in two ways. High viscosity can improve the adherence of oil on to the sorbent surface which increases the sorption capacity. On the other hand, viscous oils are difficult to penetrate into the inner surfaces of the sorbents [51]. Key properties of several oils and organic solvents are listed in Table 4. The sorption capacity of the sorbents shown in Fig. 11 agrees with the decreasing tendency of oil viscosities. The composite beads show higher sorption capacities for paraffin and olive oils with higher viscosities compared to *n*-hexane and toluene which

Table 2
Bulk density of the ZIF-8/PES composite beads in comparison with ZIF-8 and PES.

Material	Bulk density (g.cm^{-3})
ZIF-8	0.36
ZIF/PES-4	0.26
ZIF/PES-2	0.18
ZIF/PES-1	0.17
ZIF/PES-0.5	0.053
PES	0.035

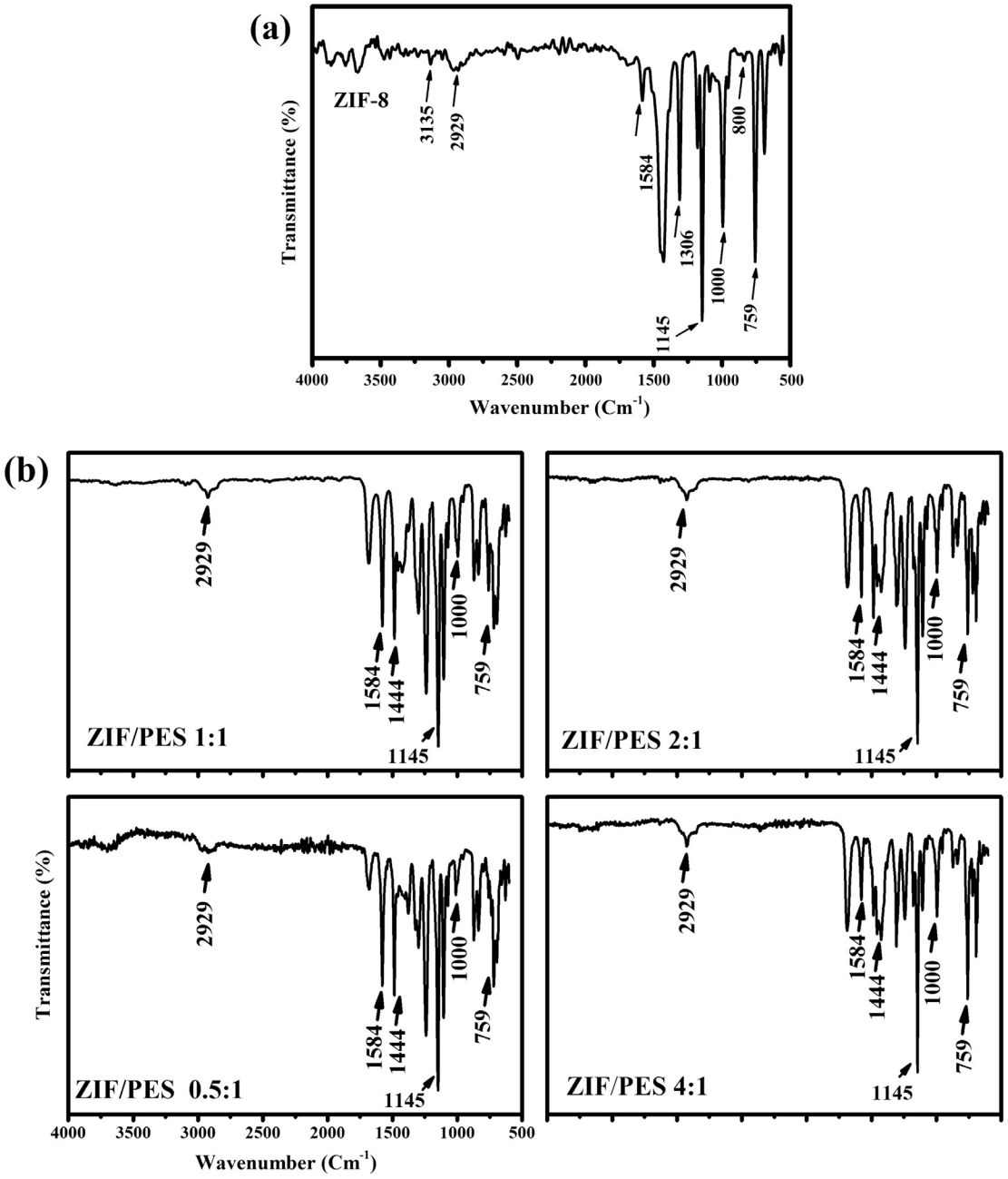

Fig. 7. FTIR spectra of ZIF-8 (a) and ZIF/PES beads with different ZIF/PES ratios (b)

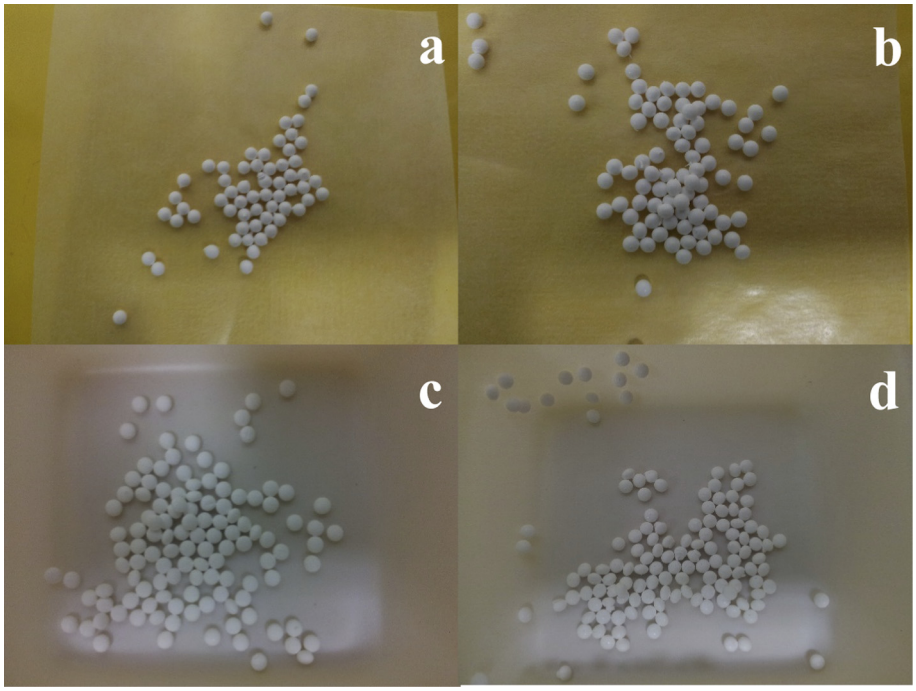

Fig. 8. Digital images of ZIF-8 composite beads: ZIF/PES-0.5 (a), ZIF/PES-1 (b), ZIF/PES-2 (c) ZIF/PES-4 (d)

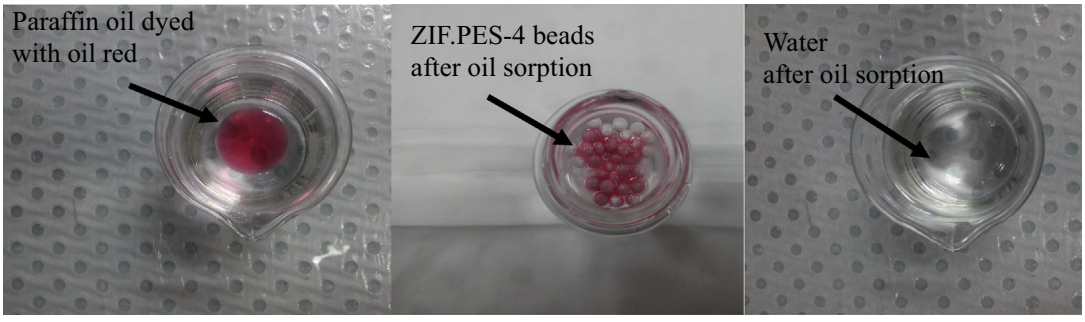

Fig. 9. Digital images of ZIF-8 composite beads floating on the surface of water and paraffin oil sorption marked with oil red.

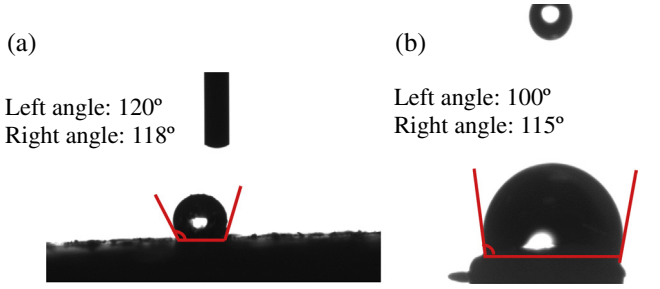

Fig. 10. The water contact angle of ZIF-8 powder (left angle: 120° and right angle: 118°) (a) and ZIF/PES-4 (left angle: 100° and right angle: 115°) (b)

have much lower viscosities. The sorption of *n*-hexane is still comparable with the sorption of paraffin and olive oils despite the low viscosity of *n*-hexane, probably due to the very small kinetic diameter of this solvent which makes its penetration into the ZIF-8 pores much easier. Although the oil diffusion rate is inversely proportional to the viscosity, the hydrophobic nature of ZIF-8 particles and the large pores on the surface of the beads at high ZIF-8 loading overcome the penetration difficulty leading to high sorption capacities.

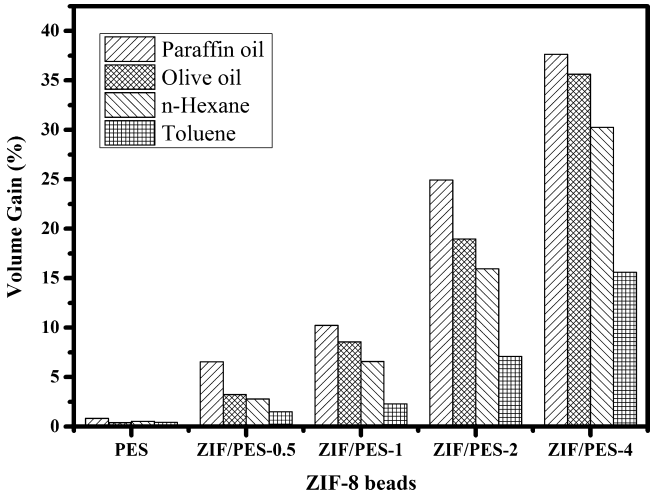

Fig. 11. Oil sorption capacities of ZIF-8 composite beads for oils and organic solvents in terms of volume gain.

It is necessary for an adsorbent to be regenerated and reused in the adsorption process. The reusability of the beads for organic solvents was tested by heating the beads up to the normal boiling

Table 3
Comparison of oil/organic sorption capacities of different sorbents.

Sorbent	Long-chain oil ($mg.g^{-1}$)	Sorbent density ($g.cm^{-3}$)	Reference
ZIF/PES-4 composite beads	1260	0.26	This study
Pure ZIF-8 powder	3000	NA[a]	[36]
Pure ZIF-8 powder	2650	0.36	This study
UHMOF-100	2000	NA	[52]
HFGO@ZIF-8	200	NA	[53]
Sponge@HFGO@ZIF-8	2000	NA	[53]
HKUST-1 (MOF)	260	1.22	[54]
Hollow carbon beads	1557	0.2	[24]
Carbon/TiO_2 beads	1151.7	0.6	[55]
Activated carbon	50	NA	[54]
Activated carbon	167	NA	[7]
Activated carbon	300	2	[56]
Bentonite	378	1.15	[57]
Zeolite	55–100	1.6–2.4	[8]

Table 4
Density and normal boiling points of the organic compounds.

Organic compounds	Density ($g.cm^{-3}$)	Viscosity (cp)	Normal boiling point (°C)
Paraffin oil	0.89	20	260–450
Olive oil	0.9	69	300
n-Hexane	0.65	0.3	69
Toluene	0.86	0.59	110

point of *n*-hexane (68 °C) and toluene (110 °C) for one hour. The beads showed almost one hundred percent regeneration efficiency. However, the normal boiling point of paraffin oil is in the range of 260-450 °C, therefore, the solvent washing method was utilized to regenerate the composite beads for desorbing paraffin oil form the beads. Although heat treatment is a more effective method in recycling adsorbents, due to the low stability of ZIF-8 (300 °C) and polymer framework (185 °C) at high temperatures, the solvent method was utilized for recycling of the composite beads for paraffin oil.

The regeneration test was done for the composite beads after paraffin oil sorption and the used beads were washed with ethanol. The regeneration results are shown in Fig. 12(a) demonstrating that composite beads are able to retain 88 percent of the original oil sorption after 5 regeneration cycles. This indicates that solvent washing is a simple and effective method for the regeneration of the composite beads and can be considered as an alternative to heat treatment for recycling purposes. The XRD patterns of the ZIF-8 composite beads before oil sorption and after regeneration are illustrated in Fig. 12(b) showing that the XRD pattern of the beads after 5 cycles of regeneration is similar to the beads before oil sorption. This indicates the composite beads have a stable structure and can be reused for oil sorption.

Table 3 summarizes the oil sorption capacities of different kind of sorbents for comparison. The capacity of the ZIF-8 composite beads was converted to weight basis from volume basis to be comparable with the sorption capacities from literature. The table shows that the ZIF composite beads can compete with other sorbents for oil sorption and have very high sorption capacities.

The ZIF-8 composite beads have lower sorption capacities compared with the pure ZIF-8 powder, which is due to the fact that the beads include polymer in their matrices and the bead framework is composed of a mixture of ZIF-8 particles as well as polymer. Moreover, the ZIF-8 powder has more accessible surface area to the oils and organic solvents since the particles are nano-sized and have high exposure to the pollutant molecules. The sorption capacity of ZIF-8 powder is based on the weight of pure ZIF-8 powder while the sorption capacity of composite beads is based on the weight of

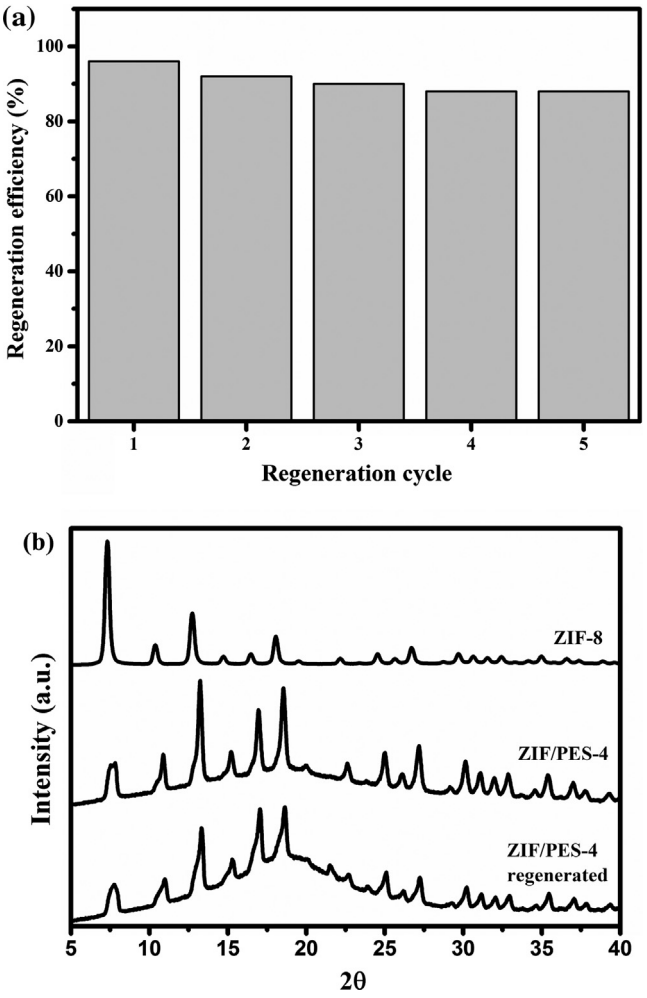

Fig. 12. Recyclability of ZIF-8/PES composite beads. Regeneration efficiency of the composite beads (a) and XRD patterns of ZIF-8/PES beads before and after oil sorption.

the ZIF/PES composite beads. It is also shown that the ZIF-8/PES composite beads have greater oil sorption capacities compared with HKUST-1 metal organic framework. The composite beads also exhibit appropriate sorption capacities in comparison with UHMOF-100 and HFGO@ZIF-8 considering the fact that the above-mentioned sorbents are difficult to handle and recycle. Although pure ZIF-8, UHMOF-100 and HFGO@ZIF-8 exhibit higher sorption capacities compared to ZIF-8 composite beads, they are in powder form which is simply not useful for practical oil spillage clean-up purposes. The composite beads in this study have the advantage of keeping ZIF-8 particles in a rigid, robust and stable framework to enable simple handling during oil sorption and recycling processes.

In comparison with hollow carbon beads and carbon/TiO_2 beads, the ZIF-8 composite beads still show good sorption properties. In particular, when compared with natural sorbents like activated carbon, zeolite and bentonite, the ZIF-8/PES beads exhibit much higher sorption capacities. It is worth mentioning that ZIF-8 composite beads present a very low bulk density compared to the other sorbents listed in Table 2. HKUST-1 metal organic framework has bulk density of 1.22 $g.cm^{-3}$ which is higher than water density. The bulk density of zeolite is in the range of 1.6–2.4 $g.cm^{-3}$ and that of activated carbon is 2 $g.cm^{-3}$, which are much higher than the bulk density of ZIF/PES-4 beads reported in this study. The bulk density of the ZIF-8 composite beads is even lower than the carbon/TiO_2 beads and close to that of hollow carbon

beads. As mentioned previously, the natural sorbents mostly exhibit poor buoyancy which is not suitable for cleaning oil spills from the surfaces of water. These natural sorbents cannot float on the surface of water and therefore have limitation regarding with oil spill removals. These materials do not benefit from simultaneous high oil sorption capacity and good buoyancy. In most cases, either sorption capacity or buoyancy is sacrificed. In contrast, ZIF-8 composite beads benefit from both high sorption uptake and suitable buoyancy which makes them interesting for oil spillage uptake. The ZIF-8/PES beads have bulk densities even lower than ZIF-8 powder (0.36 $g.cm^{-3}$).

It is worth noting that in comparison with other beads which are reported for oil spill removal like hollow carbon beads and carbon/TiO_2 beads, ZIF-8/PES beads have the advantage of being prepared from a simple one step method, while the carbon beads are prepared via a second carbonization step which is time and energy consuming. The HFGO@ZIF-8 and sponge@HFGO@ZIF-8 are also prepared from several complicated steps which restricts practical application. The stability of the beads after oil sorption experiments was also evaluated by XRD analysis. It can be observed from Fig. 10 that the prepared beads exhibit stability after oil adsorption since the XRD pattern is quite similar before and after oil adsorption.

Therefore, the high oil sorption capacity along with the rigidity and robustness of the beads frameworks, plus low bulk density and excellent buoyancy make these composite beads suitable candidates for oil spill clean-up in practical purposes. In addition, the simple one step method for fabrication of ZIF-8 is superior to other complicated techniques utilized for preparing the other synthetic sorbent materials.

4. Conclusions

The ZIF-8 composite beads were prepared successfully using the phase inversion method. This is a very simple and straight forward technique and the prepared ZIF-8/PES beads are quite rigid and stable. The SEM and XRD analyses confirmed the uniform incorporation of ZIF-8 particles in the polymer matrix. The surface area of the ZIF-8/PES composite beads increased with increasing the ZIF-8 loading up to 1030.6 m^2/g close to the surface area of pure ZIF-8 (1384.2 m^2/g). The oil sorption experiments showed that the composite beads are capable of adsorbing oils and organic solvents efficiently. The oil adsorption capacity of the ZIF-8/PES-4 composite beads was 1260 mg/g which is significantly higher than that of natural adsorbents such as activated carbon, zeolite and bentonite with adsorption capacities of 300, 100 and 378 mg/g, respectively. The ZIF-8/PES-4 composite beads also exhibited a very low bulk density (0.26 g/cm^3) in comparison with ZIF-8 powder with a bulk density of 0.36 g/cm^3 as well as natural adsorbents such as activated carbon, zeolite and bentonite with bulk densities of 2, 1.6 and 1.15 g/cm^3, respectively. This low bulk density of the ZIF-8/PES beads resulted in excellent buoyancy compared with the natural adsorbents.

The high sorption is attributed to the hydrophobicity and high surface area of the ZIF-8 particles. This study showed ZIF-8 composite beads can compete with other sorbent materials and exhibit much higher sorption capacities in comparison with activated carbon. The synthesized composite beads are easy to handle and recycle and can retain up to 88 percent of the oil sorption capacity after five regeneration cycles.

Acknowledgement

This work was supported by the Australian Research Council through a Future Fellowship (Huanting Wang, Project no. FT100100192). The authors gratefully acknowledge the use of electron microscopes at Monash Centre for Electron Microscopy.

Appendix A. Supplementary material

Supplementary data associated with this article can be found, in the online version, at http://dx.doi.org/10.1016/j.jcis.2017.01.006.

References

[1] H. Bi, X. Xie, K. Yin, Y. Zhou, S. Wan, L. He, F. Xu, F. Banhart, L. Sun, R.S. Ruoff, Spongy graphene as a highly efficient and recyclable sorbent for oils and organic solvents, Adv. Funct. Mater. 22 (2012) 4421–4425.
[2] Y. Gao, Y.S. Zhou, W. Xiong, M. Wang, L. Fan, H. Rabiee-Golgir, L. Jiang, W. Hou, X. Huang, L. Jiang, J.-F. Silvain, Y.F. Lu, Highly efficient and recyclable carbon soot sponge for oil cleanup, ACS Appl. Mater. Interf. 6 (2014) 5924–5929.
[3] S. Kabiri, D.N.H. Tran, T. Altalhi, D. Losic, Outstanding adsorption performance of graphene–carbon nanotube aerogels for continuous oil removal, Carbon 80 (2014) 523–533.
[4] X. Dong, J. Chen, Y. Ma, J. Wang, M.B. Chan-Park, X. Liu, L. Wang, W. Huang, P. Chen, Superhydrophobic and superoleophilic hybrid foam of graphene and carbon nanotube for selective removal of oils or organic solvents from the surface of water, Chem. Commun. 48 (2012) 10660–10662.
[5] S.B. Ummalyma, R.K. Sukumaran, Cultivation of microalgae in dairy effluent for oil production and removal of organic pollution load, Bioresour. Technol. 165 (2014) 295–301.
[6] J. Zhao, W. Ren, H.-M. Cheng, Graphene sponge for efficient and repeatable adsorption and desorption of water contaminations, J. Mater. Chem. 22 (2012) 20197–20202.
[7] A.L. Ahmad, S. Sumathi, B.H. Hameed, Residual oil and suspended solid removal using natural adsorbents chitosan, bentonite and activated carbon: a comparative study, Chem. Eng. J. 108 (2005) 179–185.
[8] M.A. Shavandi, Z. Haddadian, M.H.S. Ismail, N. Abdullah, Continuous metal and residual oil removal from palm oil mill effluent using natural zeolite-packed column, J. Taiwan Ins. Chem. Eng. 43 (2012) 934–941.
[9] M.O. Adebajo, R.L. Frost, J.T. Kloprogge, O. Carmody, S. Kokot, Porous materials for oil spill cleanup: a review of synthesis and absorbing properties, J. Porous. Mater. 10 (2003) 159–170.
[10] S.-J. Choi, T.-H. Kwon, H. Im, D.-I. Moon, D.J. Baek, M.-L. Seol, J.P. Duarte, Y.-K. Choi, A polydimethylsiloxane (PDMS) sponge for the selective absorption of oil from water, ACS Appl. Mater. Interf. 3 (2011) 4552–4556.
[11] A. Li, H.-X. Sun, D.-Z. Tan, W.-J. Fan, S.-H. Wen, X.-J. Qing, G.-X. Li, S.-Y. Li, W.-Q. Deng, Superhydrophobic conjugated microporous polymers for separation and adsorption, Energy Environ. Sci. 4 (2011) 2062–2065.
[12] Q. Zhu, Y. Chu, Z. Wang, N. Chen, L. Lin, F. Liu, Q. Pan, Robust superhydrophobic polyurethane sponge as a highly reusable oil-absorption material, J. Mater. Chem. A 1 (2013) 5386–5393.
[13] X. Gui, J. Wei, K. Wang, A. Cao, H. Zhu, Y. Jia, Q. Shu, D. Wu, Carbon nanotube sponges, Adv. Mater. 22 (2010) 617–621.
[14] J. Li, F. Wang, C.-Y. Liu, Tri-isocyanate reinforced graphene aerogel and its use for crude oil adsorption, J. Colloid Interf. Sci. 382 (2012) 13–16.
[15] H. Liu, C.-Y. Cao, F.-F. Wei, P.-P. Huang, Y.-B. Sun, L. Jiang, W.-G. Song, Flexible macroporous carbon nanofiber film with high oil adsorption capacity, J. Mater. Chem. A 2 (2014) 3557–3562.
[16] H.-W. Liang, Q.-F. Guan, L.-F. Chen, Z. Zhu, W.-J. Zhang, S.-H. Yu, Macroscopic-scale template synthesis of robust carbonaceous nanofiber hydrogels and aerogels and their applications, Angew. Chem. Int. Ed. 51 (2012) 5101–5105.
[17] Y. Li, S. Cheng, P. Dai, X. Liang, Y. Ke, Large-pore monodispersed mesoporous silica spheres: synthesis and application in HPLC, Chem. Commun. 1085–1087 (2009).
[18] W. Zhao, H. Chen, Y. Li, L. Li, M. Lang, J. Shi, Uniform rattle-type hollow magnetic mesoporous spheres as drug delivery carriers and their sustained-release property, Adv. Funct. Mater. 18 (2008) 2780–2788.
[19] P.M. Arnal, M. Comotti, F. Schüth, High-temperature-stable catalysts by hollow sphere encapsulation, Angew. Chem. 118 (2006) 8404–8407.
[20] M. Najafi, Y. Yousefi, A.A. Rafati, Synthesis, characterization and adsorption studies of several heavy metal ions on amino-functionalized silica nano hollow sphere and silica gel, Sep. Purif. Technol. 85 (2012) 193–205.
[21] H. Zhang, G.C. Hardy, Y.Z. Khimyak, M.J. Rosseinsky, A.I. Cooper, Synthesis of hierarchically porous silica and metal oxide beads using emulsion-templated polymer scaffolds, Chem. Mater. 16 (2004) 4245–4256.
[22] J. Yao, K. Wang, M. Ren, J. Zhe Liu, H. Wang, Phase inversion spinning of ultrafine hollow fiber membranes through a single orifice spinneret, J. Membr. Sci. 421–422 (2012) 8–14.
[23] J. Huang, K. Zhang, K. Wang, Z. Xie, B. Ladewig, H. Wang, Fabrication of polyethersulfone-mesoporous silica nanocomposite ultrafiltration membranes with antifouling properties, J. Membr. Sci. 423–424 (2012) 362–370.
[24] Y. Zeng, K. Wang, J. Yao, H. Wang, Hollow carbon beads fabricated by phase inversion method for efficient oil sorption, Carbon 69 (2014) 25–31.
[25] L. Li, J. Yao, P. Xiao, J. Shang, Y. Feng, P.A. Webley, H. Wang, One-step fabrication of ZIF-8/polymer composite spheres by a phase inversion method for gas adsorption, Colloid Polym. Sci. 291 (2013) 2711–2717.

[26] N.A. Khan, Z. Hasan, S.H. Jhung, Adsorptive removal of hazardous materials using metal-organic frameworks (MOFs): a review, J. Hazard. Mater. 244–245 (2013) 444–456.
[27] N.A. Khan, B.K. Jung, Z. Hasan, S.H. Jhung, Adsorption and removal of phthalic acid and diethyl phthalate from water with zeolitic imidazolate and metal–organic frameworks, J. Hazard. Mater. 282 (2015) 194–200.
[28] J.A. Gee, J. Chung, S. Nair, D.S. Sholl, Adsorption and diffusion of small alcohols in zeolitic imidazolate frameworks ZIF-8 and ZIF-90, J. Phys. Chem. C 117 (2013) 3169–3176.
[29] U.P.N. Tran, K.K.A. Le, N.T.S. Phan, Expanding applications of metal−organic frameworks: zeolite imidazolate framework ZIF-8 as an efficient heterogeneous catalyst for the Knoevenagel reaction, ACS Catal. 1 (2011) 120–127.
[30] C.M. Miralda, E.E. Macias, M. Zhu, P. Ratnasamy, M.A. Carreon, Zeolitic imidazole framework-8 catalysts in the conversion of CO2 to chloropropene carbonate, ACS Catal. 2 (2012) 180–183.
[31] B.K. Jung, J.W. Jun, Z. Hasan, S.H. Jhung, Adsorptive removal of p-arsanilic acid from water using mesoporous zeolitic imidazolate framework-8, Chem. Eng. J. 267 (2015) 9–15.
[32] Y.-N. Wu, M. Zhou, B. Zhang, B. Wu, J. Li, J. Qiao, X. Guan, F. Li, Amino acid assisted templating synthesis of hierarchical zeolitic imidazolate framework-8 for efficient arsenate removal, Nanoscale 6 (2014) 1105–1112.
[33] J.-Q. Jiang, C.-X. Yang, X.-P. Yan, Zeolitic imidazolate framework-8 for fast adsorption and removal of benzotriazoles from aqueous solution, ACS Appl. Mater. Interf. 5 (2013) 9837–9842.
[34] J. Li, Y.-N. Wu, Z. Li, B. Zhang, M. Zhu, X. Hu, Y. Zhang, F. Li, Zeolitic imidazolate framework-8 with high efficiency in trace arsenate adsorption and removal from water, J. Phys. Chem. C 118 (2014) 27382–27387.
[35] Z. Abbasi, E. Shamsaei, S.K. Leong, B. Ladewig, X. Zhang, H. Wang, Effect of carbonization temperature on adsorption property of ZIF-8 derived nanoporous carbon for water treatment, Microporous Mesoporous Mater. 236 (2016) 28–37.
[36] K.-Y.A. Lin, Y.-C. Chen, S. Phattarapattamawong, Efficient demulsification of oil-in-water emulsions using a zeolitic imidazolate framework: adsorptive removal of oil droplets from water, J. Colloid Interf. Sci. 478 (2016) 97–106.
[37] L.D. O'Neill, H. Zhang, D. Bradshaw, Macro-/microporous MOF composite beads, J. Mater. Chem. 20 (2010) 5720–5726.
[38] S. Aguado, J. Canivet, D. Farrusseng, Facile shaping of an imidazolate-based MOF on ceramic beads for adsorption and catalytic applications, Chem. Commun. 46 (2010) 7999–8001.
[39] T. Zhang, L. Lin, X. Zhang, H. Liu, X. Yan, Z. Liu, K.L. Yeung, Facile preparation of ZIF-8@Pd-CSS sandwich-type microspheres via in situ growth of ZIF-8 shells over Pd-loaded colloidal carbon spheres with aggregation-resistant and leach-proof properties for the Pd nanoparticles, Appl. Surf. Sci. 351 (2015) 1184–1190.
[40] X. Zhou, F. Wang, Y. Ji, W. Chen, J. Wei, Fabrication of hydrophilic and hydrophobic sites on polypropylene nonwoven for oil spill cleanup: two dilemmas affecting oil sorption, Environ. Sci. Technol. 50 (2016) 3860–3865.
[41] K. Zhang, R.P. Lively, M.E. Dose, A.J. Brown, C. Zhang, J. Chung, S. Nair, W.J. Koros, R.R. Chance, Alcohol and water adsorption in zeolitic imidazolate frameworks, Chem. Commun. 49 (2013) 3245–3247.
[42] P. Küsgens, M. Rose, I. Senkovska, H. Fröde, A. Henschel, S. Siegle, S. Kaskel, Characterization of metal-organic frameworks by water adsorption, Microporous Mesoporous Mater. 120 (2009) 325–330.
[43] K. Zhang, R.P. Lively, C. Zhang, R.R. Chance, W.J. Koros, D.S. Sholl, S. Nair, Exploring the framework hydrophobicity and flexibility of ZIF-8: from biofuel recovery to hydrocarbon separations, J. Phys. Chem. Lett. 4 (2013) 3618–3622.
[44] N.C. Burtch, H. Jasuja, K.S. Walton, Water stability and adsorption in metal–organic frameworks, Chem. Rev. 114 (2014) 10575–10612.
[45] L. Diestel, H. Bux, D. Wachsmuth, J. Caro, Pervaporation studies of n-hexane, benzene, mesitylene and their mixtures on zeolitic imidazolate framework-8 membranes, Microporous Mesoporous Mater. 164 (2012) 288–293.
[46] S. Eslava, L. Zhang, S. Esconjauregui, J. Yang, K. Vanstreels, M.R. Baklanov, E. Saiz, Metal-organic framework ZIF-8 films as low-κ dielectrics in microelectronics, Chem. Mater. 25 (2013) 27–33.
[47] B. Liu, M. Tu, R.A. Fischer, Metal–organic framework thin films: crystallite orientation dependent adsorption, Angew. Chem. Int. Ed. 52 (2013) 3402–3405.
[48] A. Henschel, I. Senkovska, S. Kaskel, Liquid-phase adsorption on metal-organic frameworks, Adsorption 17 (2011) 219–226.
[49] D. Peralta, G. Chaplais, A. Simon-Masseron, K. Barthelet, C. Chizallet, A.-A. Quoineaud, G.D. Pirngruber, Comparison of the behavior of metal–organic frameworks and zeolites for hydrocarbon separations, J. Am. Chem. Soc. 134 (2012) 8115–8126.
[50] C.D. Baertsch, H.H. Funke, J.L. Falconer, R.D. Noble, Permeation of aromatic hydrocarbon vapors through silicalite−zeolite membranes, J. Phys. Chem. 100 (1996) 7676–7679.
[51] J. Wu, N. Wang, L. Wang, H. Dong, Y. Zhao, L. Jiang, Electrospun porous structure fibrous film with high oil adsorption capacity, ACS Appl. Mater. Interf. 4 (2012) 3207–3212.
[52] S. Mukherjee, A.M. Kansara, D. Saha, R. Gonnade, D. Mullangi, B. Manna, A.V. Desai, S.H. Thorat, P.S. Singh, A. Mukherjee, S.K. Ghosh, An ultrahydrophobic fluorous metal–organic framework derived recyclable composite as a promising platform to tackle marine oil spills, Chem. Eur. J. 22 (2016) 10937–10943.
[53] K. Jayaramulu, K.K.R. Datta, C. Rösler, M. Petr, M. Otyepka, R. Zboril, R.A. Fischer, Biomimetic superhydrophobic/superoleophilic highly fluorinated graphene oxide and ZIF-8 composites for oil–water separation, Angew. Chem. Int. Ed. 55 (2016) 1178–1182.
[54] K.-Y.A. Lin, H. Yang, C. Petit, F.-K. Hsu, Removing oil droplets from water using a copper-based metal organic frameworks, Chem. Eng. J. 249 (2014) 293–301.
[55] X. Gu, K. Zhou, Y. Li, J. Yao, Millimeter-sized carbon/TiO_2 beads fabricated by phase inversion method for oil and dye adsorption, RSC Adv. 6 (2016) 16314–16318.
[56] M.A. Lillo-Ródenas, D. Cazorla-Amorós, A. Linares-Solano, Behaviour of activated carbons with different pore size distributions and surface oxygen groups for benzene and toluene adsorption at low concentrations, Carbon 43 (2005) 1758–1767.
[57] K. Okiel, M. El-Sayed, M.Y. El-Kady, Treatment of oil–water emulsions by adsorption onto activated carbon, bentonite and deposited carbon, Egypt. J. Petrol. 20 (2011) 9–15.